Ann. Geophys., 29, 1287–1293, 2011
www.ann-geophys.net/29/1287/2011/
doi:10.5194/angeo-29-1287-2011


Annales Geophysicae

# Remote sensing planetary waves in the midlatitude mesosphere using low frequency transmitter signals

**E. D. Schmitter**

University of Applied Sciences Osnabrueck, 49076 Osnabrueck, Germany

Received: 15 April 2011 – Revised: 4 July 2011 – Accepted: 18 July 2011 – Published: 20 July 2011

**Abstract.** Very low and low radio frequency (VLF/LF) propagation responds sensitively to the electron density distribution in the lower ionosphere (upper mesosphere). Whereas propagation paths crossing subpolar and polar regions are frequently affected by forcing from above by particle precipitations, mid- and lowlatitude paths let forcing from below be more prominent. Our observations (2009–2011) show, that the low frequency propagation conditions along the midlatitude path from Sicily to Germany (52° N 8° E) using the NSY 45.9 kHz transmitter (37° N 14° E) prove to be a good proxy of mesosphere planetary wave activity along the propagation path. High absorption events with VLF/LF propagation correlate to the well known winter time D-layer anomaly observed with high frequency (HF) radio waves. VLF/LF propagation calculations are presented which show that the radio signal amplitude variations can be modeled by planetary wave modulated collison frequency and electron density profiles. The other way around wave pressure amplitudes can be inferred from the VLF/LF data.

**Keywords.** Ionosphere (Ionosphere-atmosphere interactions)

## 1 Introduction

Planetary waves are disturbances in the atmosphere (with respect to wind and pressure, but also temperature variations) with zonal wavelengths at the scale of the earths radius. They can be forced in the troposphere for example by topography or land-sea temperature differences but can also exist as free resonant traveling waves. These waves are strongly related to global weather (formation of cyclones, anticyclones, mid-latitude depressions) and their variability is suggested to be a signature of possible climatic changes (Pogoreltsev et al., 2009). Under certain conditions which for the stationary wave case are approximated by the Charney-Drazin criterion (Charney and Drazin, 1961): not too strong eastward background winds and long horizontal wavelengths) planetary waves vertically penetrate to the stratosphere and also up to the mesosphere where they can affect the ionosphere (Lastovicka et al., 1994; Borries et al., 2007; Brown and John, 1979; Haldoupis and Pancheva, 2002; Haldoupis et al., 2004). During the Northern Hemisphere winter months planetary wavenumber one is large and variable in the mesosphere and we found further hints that the D-layer winter anomaly (unusually strong absorption of radio waves in the ionosphere, not related to solar activity (Appleton and Piggott, 1954; Lauter and Schaening, 1970; Lauter et al., 1984; Taubenheim, 1971), is correlated to planetary wave activity.

In the next section we describe the data related to planetary wave activity and later on the low frequency radio propagation model. The last chapter presents the main conclusions.

*Correspondence to:* E. D. Schmitter
(e.d.schmitter@hs-osnabrueck.de)

## 2 The data correlating with planetary wave activity

Very low and low frequency propagation responds sensitively to electron density and collision frequency profile changes in the mesosphere/ionosphere especially in the 70–80 km height range. In addition to forcing from above (day-night solar flux variation, X-rays and particle precipitations) the plasma conditions in this height range are also subject to forcing from below.

For remote sensing the mesosphere and lower ionosphere we monitor the signal amplitude of (very) low frequency MSK (Minimum Shift Keying) transmitters. The transmitter station with call sign NSY (45.9 kHz) at Niscemy, Sicily (37.13° N 14.44° E, $L = 1.4$) usually transmits continously with few dropouts.

Published by Copernicus Publications on behalf of the European Geosciences Union.

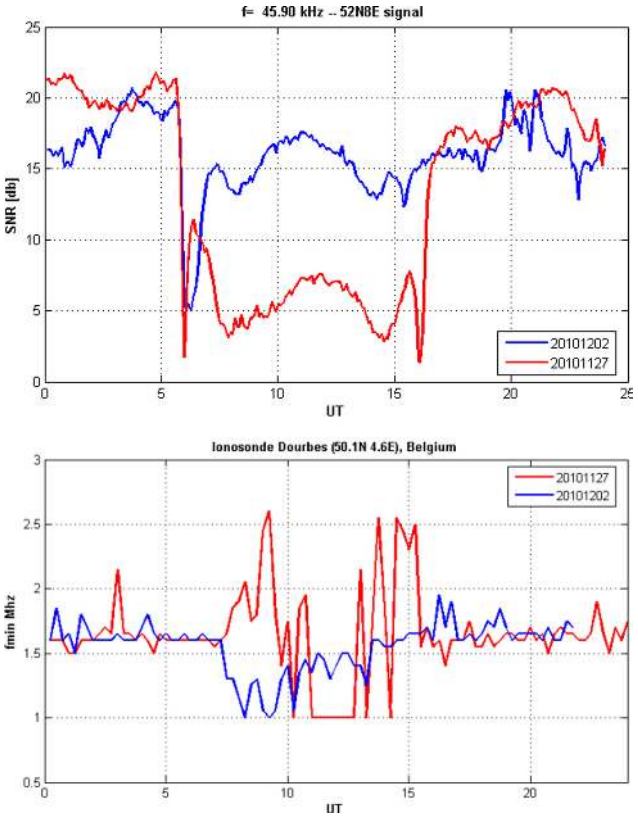


**Fig. 1.** Forcing from below: winter anomaly (strong absorption) during daytime for VLF/LF and HF radio waves; top: VLF/LF log amplitude (signal to noise ratio, dB), 45.9 kHz, (NSY-52N8E, red: 27 November 2010) cp. to nearby day with low absorption (blue 2 December 2010); bottom: $f_{\min}$ (minimum frequency of ionogram echoes) for the same days from the ionosonde (URL: http://digisonde.oma.be) at Dourbes, Belgium (50.1° N, 4.6° E), high $f_{\min}$ indicating strong HF absorption.

We monitor at a midlatitude location (52° N, 8° E, $L = 2.2$) with a great circle distance to the transmitter of 1730 km. The receiver uses a coil with a ferrite core as sensor for the horizontal magnetic field component of the radio signal. The broadband preamplified signal is fed via a soundcard into a computer, where the transmitter signal is extracted via Fast Fourier Transform (FFT) and further analysed.

The blue traces in Fig. 1 show the VLF/LF signal from NSY (top) and (bottom) the minimum ionogramm echo frequency $f_{\min}$ from the Dourbes ionosonde (Belgium, 50.1° N, 4.6° E) at a low absorption winter day (2 December 2010), the red traces a day over anomaly (strong absorption) condition a few days earlier (27 November 2010) we relate to "forcing from below" (see below). Just to illustrate a typical "forcing from above" situation Fig. 2 shows 2 signal traces with the red curve displaying a night time particle precipitation event on the propagation path from the NRK transmitter (Iceland, 37.5 kHz) to (52° N 8° E), for details see Schmitter (2010).

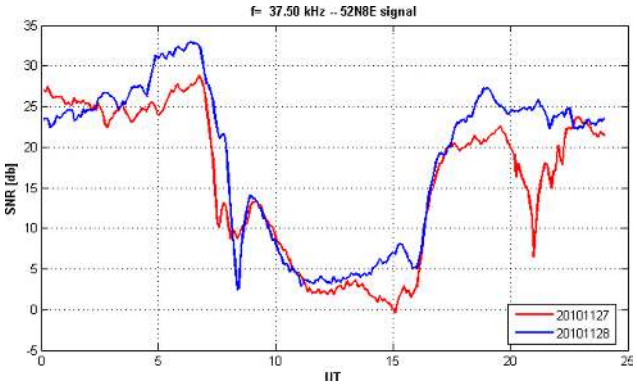


**Fig. 2.** Forcing from above: subauroral particle precipitation during nighttime (red: 27 November 2010) cp. to (blue: 28 November 2010). Path: NRK, Iceland – 52° N 8° E.

Because temperature variance can be used as a proxy for atmospheric wave activity we use mesosphere kinetic temperature data from the SABER (Sounding of the Atmosphere using Broadband Emission Radiometry) instrument as a correlation reference (LEVEL2A data product from saber.gats-inc.com). SABER was launched onboard the TIMED (Thermosphere-Ionosphere-Mesosphere-Energetics and Dynamics) satellite in 2001. Vertical profiles of kinetic temperature are derived from broadband measurements of $CO_2$ 15 µm and 4.3 µm limb emission (Mertens et al., 2004).

The upper trace in Fig. 3 is the plot of the NSY signal log. amplitude difference between local noon and midnight (in each case averaged over 2 h) for one and a half years from 1 August 2009 to 31 March 2011. Below that we see the SABER mesosphere kinetic temperature (70–80 km average) for the region 47–52° N, 6–12° E which contains the receiver oriented half of the NSY propagation path. We note the larger variations on a days to weeks scale during winter time (days 60–200: October 2009–February 2010 and days 400–560: October 2010–February 2011) compared to summer time. This is more prominently seen with the kinetic temperature but also clearly present in the VLF/LF data.

Whereas our main point for the whole time range is the increased variance in both data sets (VLF, 70–80 km averaged kinetic temperature) during winter time, within the second winter period we find some remarkable common trends (1 October 2010–31 December 2010), cp. Fig. 4.

The 2 marks in Fig. 4 (top) refer to the VLF/LF signal amplitude plots in Fig. 1. The bottom trace of Fig. 4 displays HF absorption data from the Dourbes ionosonde (Belgium, 50.1° N, 4.6° E). Plotted is (4 Mhz – $f_{\min}$), with $f_{\min}$ being the minimum ionogramm echo frequency which is large during strong absorption. Its course shows common trends of VLF/LF and HF absorption time ranges. Examining the geomagnetic Ap index for the time period in question (Fig. 3, bottom) shows no significant correlation to geomagnetic activity, endorsing "forcing from below" for the time range in

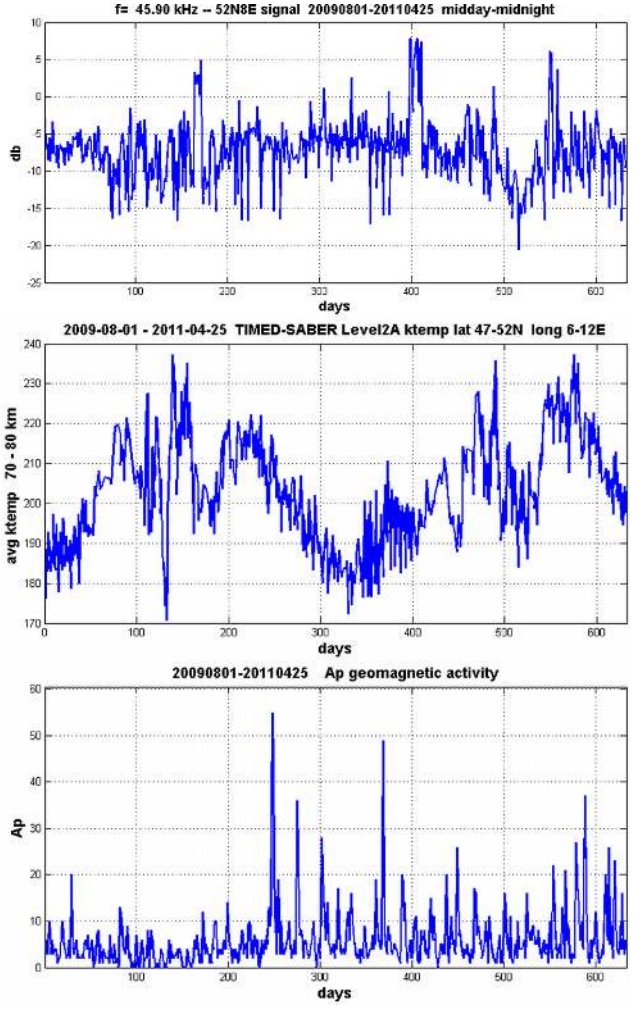


**Fig. 3.** Top: NSY log amplitude difference midday-midnight (2 h averages); Note the larger variations on a days to weeks scale during winter time (days 60–200: October 2009–February 2010 and days 400–560: October 2010–February 2011) compared to summer time – more prominently seen with the kinetic temperature but also clearly present in the VLF/LF data. Middle: SABER mesosphere kinetic temperature: 70–80 km average for the region 47–52° N, 6–12° E (containing the Rx oriented half of the propagation path) within 1 August 2009–25 April 2011. Bottom: The Ap-index for the same time range exhibits no significant correlation to the VLF/LF or kinetic temperature data.

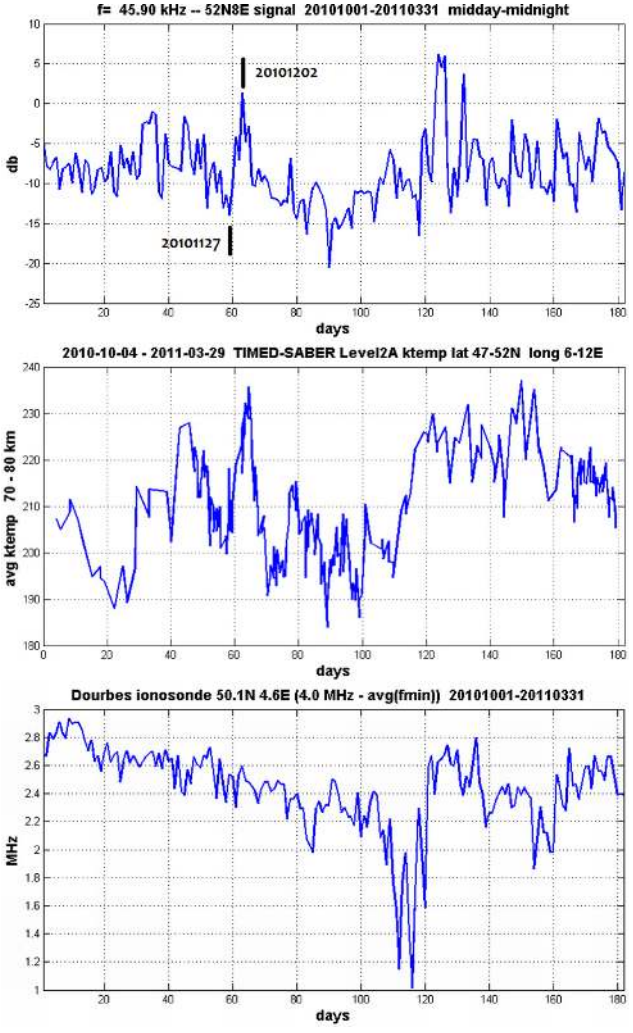


**Fig. 4.** Top: NSY log amplitude difference midday-midnight (2 h averages); the 2 marks refer to the radio signal amplitude plots in Fig. 1. Middle: SABER mesosphere kinetic temperature: 70–80 km average for the region 47–52° N, 6–12° E (containing the Rx oriented half of the propagation path) during winter 1 September–31 March 2011. Note some correlating trends. Bottom: HF absorption data from the Dourbes ionosonde (Belgium, 50.1° N, 4.6° E). Plotted is (4 Mhz – $f_{\min}$), $f_{\min}$: minimum ionogramm echo frequency; $f_{\min}$ is large during strong absorption events.

question. It may be expected however that geomagnetic influence will increase with the ongoing solar cycle.

To quantify our propositions Fig. 5 contains the Fourier spectra of the data in Fig. 4 which we discuss with regard to periods >5 days. With the VLF data the peaks at 7, 7.5 days period are a consequence of weekly transmitter drop outs (presumably maintenance). Clearly visible are 13–14 days as well as 20 and 26 days periods. With the SABER temperature data we find periods of 12.5 and 15 days as well as a broad maximum at 22–25 days period. The Dourbes $f_{\min}$ absorption data show periods of 13, 20 and 26 days (broad maximum).

With regard to the common range of periods between about 13 and 15 days a relation to quasi 16 day period planetary waves seems likely. For the latter there is a sound body of observational evidence (Madden, 1978; Mitchell et al., 2002).

We note that high radio wave absorption correlates to low temperature in the 70–80 km height range. With regard to radio wave propagation modeling (next chapter) we also note that lower temperature corresponds to higher neutral density

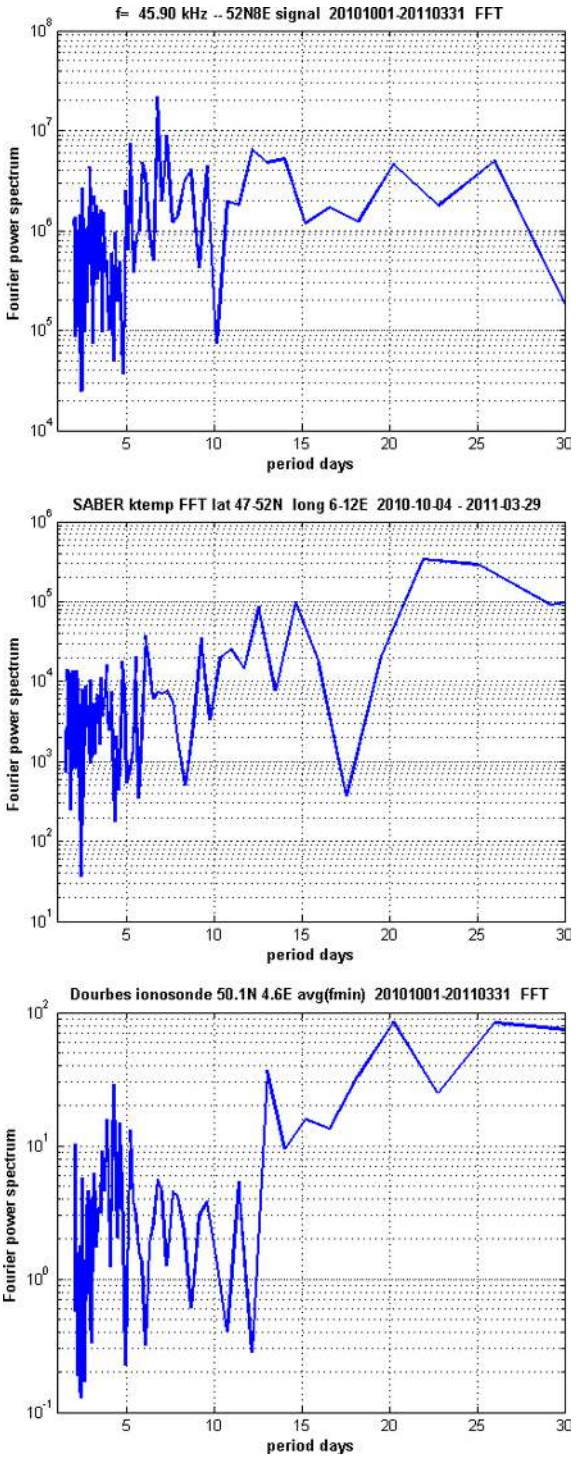


**Fig. 5.** Fourier power spectra of the data in Fig. 4. Looking at periods longer than 5 days we note: With the VLF data (top) the peaks at 7, 7.5 days period are a consequence of weekly transmitter drop outs (presumably maintenance). Clearly visible are 13-14 days as well as 20 and 26 days periods. With the SABER temperature data (middle) we find periods of 12.5 and 15 days as well as a broad maximum at 22–25 days period. The Dourbes $f_{\min}$ absorption data (bottom) show periods of 13, 20 and 26 days (broad maximum).

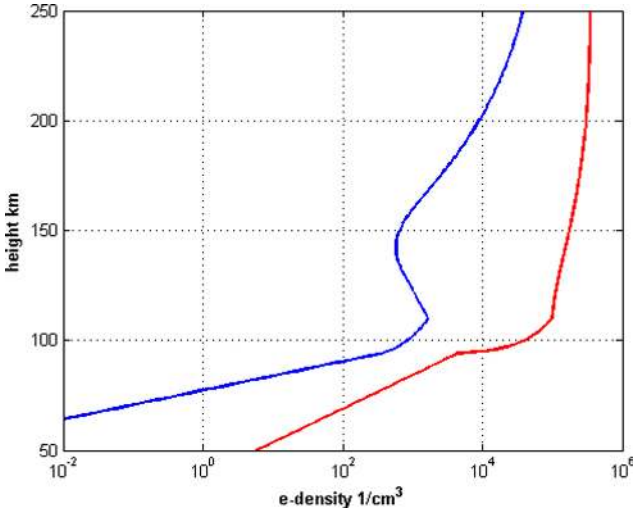


**Fig. 6.** Undisturbed electron-density profiles for midnight (blue; D-layer parameters: $h' = 87$ km, $\beta = 0.5$) and noon (red; D-layer parameters: $h' = 74$ km, $\beta = 0.3$).

which amounts to increased electron collision frequency (see below).

## 3 Long radio wave propagation modeling

For the propagation model calculations we use the Long-Wavelength Propagation Capability (LWPC) code (Ferguson, 1989) complemented by our electron density and collision frequency profiles and a suitable day-night transition scheme.

Electron density up to 95 km height is parametrized for the ionosphere D-layer according to Wait and Spies (1964) by $n_e(h) = 1.43 \times 10^7 \exp(-0.15h')\exp((\beta - 0.15)(h - h'))\,\mathrm{cm}^{-3}$ and above that by interpolating to a 2-layer Chapman profile, cp. Fig. 6. D-layer parameters for midnight are $h' = 87$ km, $\beta = 0.5$ and $h' = 74$ km, $\beta = 0.3$ for noon. All parameters defining the electron density profile are interpolated between the midnight and noon values using a power of cos(sun zenith angle) and an asymmetric night-day/day-night transition (Fig. 8). This parametrization proves sufficient for the calculation of mean day and night signal levels as well as the terminator positions.

The collision frequencies ($s^{-1}$) used in our model have been taken from Kelley (2009): $\nu_{\mathrm{in}} = 2.6 \times 10^{-9} n_{\mathrm{n}} A^{-1/2}$ for the ion-neutral collision frequency, $\nu_{\mathrm{e}} = 5.4 \times 10^{-10} n_{\mathrm{n}} T_{\mathrm{e}}^{1/2} + (34 + 4.18 \ln(T_{\mathrm{e}}^3/n_{\mathrm{e}}))\, n_{\mathrm{e}} T_{\mathrm{e}}^{-3/2}$ for the sum of the electron-neutral and electron-ion collision frequency. $n_{\mathrm{n}}$, $n_{\mathrm{e}}$ are the neutral and electron densities per cubic centimeter, $A$ is the mean neutral molecular mass and $T_{\mathrm{e}}$ the electron temperature in Kelvin. Figure 7 shows a plot of the undisturbed collision frequency height profiles. The day-night difference of $\nu_{\mathrm{e}}$ above about 120 km height

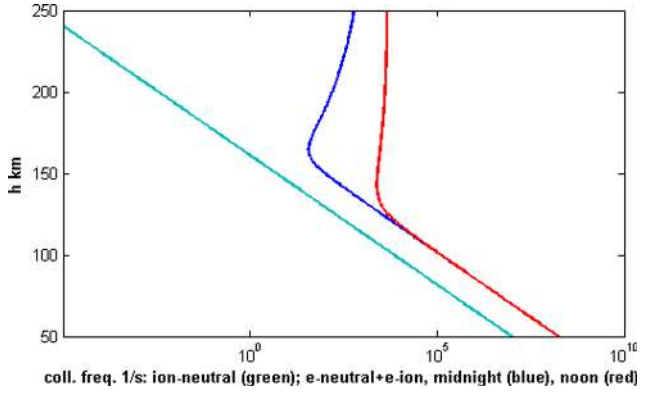


**Fig. 7.** Undisturbed collision frequency profiles. With these profiles (and those displayed in Fig. 6) modulated by the atmospheric waves (see text) the signal amplitudes in Fig. 9 have been computed.

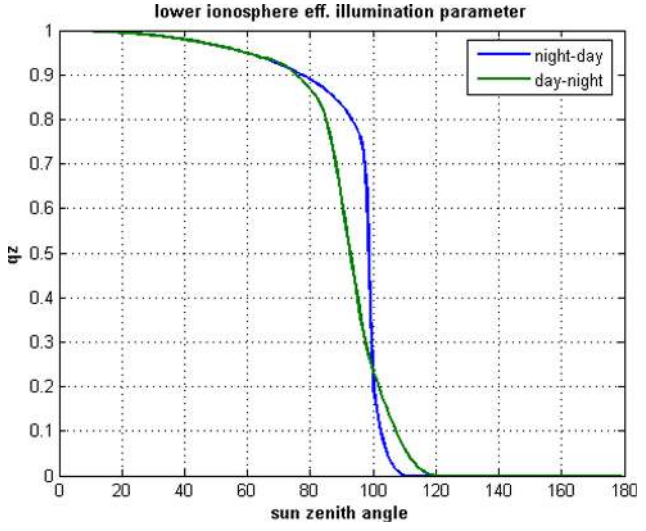


**Fig. 8.** Interpolation function for the electron density profile night/day parameters.

results from the electron-ion collision part dominating at greater heights – however, merely relevant for low frequency propagation. Below 120 km electron-neutral collisions dominate day and night. In the lower ionosphere electron neutral collision frequency is $\nu_e = 5.4 \times 10^{-10} n_n T_e^{1/2}$ and the neutral number density can be expressed by the pressure $p$ and the neutral temperature $T_n$ using the ideal gas equation: $n_n \times 10^6 = pN_A/(RT_n)$ with universal gas constant $R$ and Avogadro constant $N_A$ to yield: $\nu_e = 3.9 \times 10^7 pT_e^{1/2}/T_n$. Using $p(h) = 1.013 \times 10^5 e^{-0.145h}$ (Pascal) for the average pressure profile and assuming thermal equilibrium, i.e. $T := T_e = T_n$ the electron neutral collision frequency profile can be calculated. $T = 210$ K has been used as averaged temperature value (cp. SABER temperatures) for the relevant height range 65–85 km.

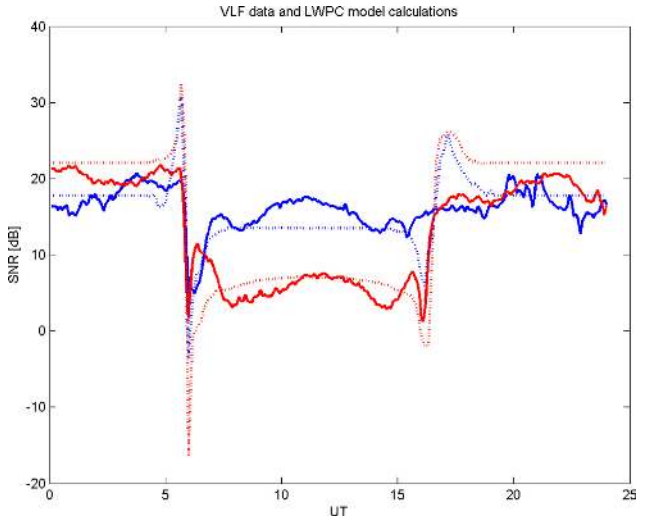


**Fig. 9.** VLF data and (cp. Fig. 1) and propagation modeling (dotted lines) with LWPC: radio signal amplitude with low (day over) absorption condition (blue, low day-night difference; 20 % reduced collision frequency amplitude and 5 % increased electron density amplitude between 65 and 85 km height with respect to undisturbed electron density and collision frequency profiles (see text)) and high (day over) absorption condition (red curve, high day-night difference; 30 % increased collision frequency amplitude and 5 % reduced electron density amplitude between 65 and 85 km height).

Atmospheric waves above a given location modulate density (and pressure) as a function of time and height and therefore directly modulate the collision frequency profile. Following Lastovicka et al. (1994) this takes place mainly in a height range of 65-85 km and we take this into account by modifying the electron collision frequency according to: $f_c(t,h) = f_c(h)(1+d_c\cos(2\pi\ t/P)\sin(\pi(h-65)/(85-65))$ with $f_c(h)$ the undisturbed profile, $d_c$ the relative disturbance amplitude (typically $d_c = 0.15-0.3$, i.e. 15–30 %) and $P$: planetary wave period. A high neutral density phase causing high collision frequency and high radio absorption values is related to a low temperature phase and vice versa. This is in agreement with the observations (Fig. 4). We assert that the maximum temperature amplitudes in Figs. 3 and 4 are of the order of 10–20 %. The neutral density variation indirectly can modulate also electron density. Using an electron density profile modified between 65–85 km height according to $n_e(t,h) = n_e(h)(1-d_e\cos(2\pi\ t/P)\sin(\pi(h-65)/(85-65))$ with $d_e = 0.05$, i.e. 5 %, increases the effects caused by the collision frequency modulation. Larger $d_e$-values in the model diminish quantitative concordance with our observational results. Note that electron density and collision frequency are out of time phase bei 180 degrees. This is in accordance with the findings of Lastovicka et al. (1994). Reasons for reduced electron density during periods of increased neutral density in the height range in question are: less ionization because of larger opacity and

increased recombination rates. With respect to increasing opacity we note that the ionization rate of the most relevant ionizing process in the D-layer, NO-ionization by solar Lyman $\alpha$ radiation, drops exponentially with increasing total content of molecular oxygen along a fixed vertical line of sight (Kockarts, 2002). Figure 9 illustrates model calculations for two rather extreme situations as with 27 November and 2 December 2010 (cp. Fig. 1) overlayed to the recorded VLF/LF data (cp. Fig. 1). Computed are the radio signal field strengths for 45.9 kHz propagation along the path (NSY-52N8E), 1 December, and scaled to the receivers signal to noise ratio (SNR(dB)). We see the results for the low (day over) absorption condition (blue, low day-night difference; 20 % reduced collision frequency amplitude and 5 % increased electron density amplitude between 65 and 85 km height with respect to base ionosphere parameters (undisturbed profiles) as described earlier) and for the high (day over) absorption condition (red curve, high day-night difference; 30 % increased collision frequency amplitude and 5 % reduced electron density amplitude between 65 and 85 km height). The results are consistent with our recordings and sensitive to variations of the given percentages. The mean day and night levels are modeled quantitatively. Detailed fluctuations can not be captured by the model and overshoots at the terminators are artifacts of the algorithm.

## 4 Conclusions

We found correlations between VLF/LF-signal amplitudes and planetary wave activity (mainly with quasi 16 day period) in the NW European midlatitude range especially during winter time and with respect to variances during the whole time window under consideration (September 2009 to April 2011). An averaging area of about 600 km squared and centered at 49.5° N 9° E is encompassed. Our VLF/LF observations as well as ionosonde HF recordings endorse the idea that planetary wave activity is a major driving force for winter time D-layer absorption effects affecting VLF, LF and HF radio waves.

Based on the results of Lastovicka et al. (1994), Lauter et al. (1984) and Taubenheim (1971) with respect to the role of electron density and collision frequency profiles during winter anomaly events we are able to quantify the variation amplitudes of these profiles by fitting them to our VLF data.

Our recordings can be modeled with collision frequency profiles with a typical 20–30 % – variation amplitude and out of time phase electron density modulation with an up to 5 % – amplitude in the mesosphere height range of 65–85 km. This result relates VLF/LF absorption variation to neutral density and pressure variations via the electron collision frequency.

Comparing the time course of our VLF/LF absorption data, especially its seasonal variance, with kinetic temperature data, suggests that we see the effect of planetary waves. Using $p = \text{const}\ \nu_e\ T^{1/2}$ and accordingly $\Delta p/p = \Delta\nu_{e/\nu_e} + 1/2\Delta T/T$ (with temperatures from SABER data) yields the relative pressure amplitudes. For our (rather extreme) example (27 November 2010 vs. 2 December 2010) using our model results and SABER temperature data we infer a 15 % pressure drop during low absorption and a 28 % pressure increase during high absorption. As increasing collision frequency goes in parallel with dropping temperature, the two contributions to $\Delta p/p$ are counteractive, with $\Delta T/T$ playing the minor role and estimates can be gained without it. To sum up, from the day-night difference of the VLF/LF signal levels using our propagation model we get the deviation of the collision frequency between 65 and 85 km height from a standard profile which in turn is directly proportional to the pressure deviation in this height range on a day to day base.

We conclude that sensing the lower ionosphere using VLF/LF transmitters proves as a useful and inexpensive proxy for atmospheric wave activity including pressure amplitude estimation in the upper mesosphere height range.

Further work will be done to confirm observational results over longer time periods and to advance models of the detailed atmospheric wave-plasma interaction (wave transformation) in the upper mesosphere.

*Acknowledgements.* Topical Editor K. Kauristie thanks J. Laštovicka and D. Lummerzheim for their help in evaluating this paper.

## References

Appleton, E. V. and Piggott, W. R.: Ionospheric Absorption Measurements during a Sunspot Cycle, J. Atmosp. Terr. Phys., 5, p. 141, 1954.

Borries, C., Jakowski, C., Jacobi, N., Hoffmann, Ch., and Pogoreltsev, A.: Spectral analysis of planetary waves seen in ionospheric total electron content (TEC): First results using GPS differential TEC and stratospheric reanalyses, J. Atmos. Solar-Terr. Phys., 69(17–18), 2442–2451, Vertical Coupling in the Atmosphere/Ionosphere System, 3rd IAGA/ICMA Workshop, doi:10.1016/j.jastp.2007.02.004, 2007.

Brown, G. M. and John, J. I.: Vertical penetration of planetary waves into the lower ionosphere, J. Atmos. Terr. Phys., 41(4), 379–385, doi:10.1016/0021-9169(79)90034-5, 1979.

Charney, J. G. and Drazin, P. G.: Propagation of planetary-scale disturbances from the lower into the upper atmosphere, J. Geophys. Res., 66, 83–109, 1961.

Ferguson, J. A.: Computer Programs for Assessments of Long-Wavelength Radio Communications, Version 2.0, Technical Document, SPAWAR Systems Center, San Diego, USA, 1998.

Haldoupis, C. and Pancheva, D.: Planetary waves and midlatitude sporadic E layers: Strong experimental evidence for a close relationship, J. Geophys. Res., 107(A6), doi:10.1029/2001JA000212, 2002.

Haldoupis, C., Pancheva, D., and Mitchell, N. J.: A study of tidal and planetary wave periodicities present in midlatitude sporadic E layers, J. Geophys. Res., 109, A02302, doi:10.1029/2003JA010253, 2004.

Kelley, M. C.: The Earths Ionosphere, PLasma Physics and Electrodynamics, chapter 2.2, Academic Press, second edition, 2009.

Kockarts, G.: Aeronomy, a 20th Century emergent science: the role of solar Lyman series, Ann. Geophys., 20, 585–598, doi:10.5194/angeo-20-585-2002, 2002.

Lastovicka, J., Ebel, A., and Ondraskova, A.: On the transformation of planetary waves of tropospheric origin into waves in radio wave absorption in the lower ionosphere, Studia Geophysica et Geodaetica, 38(1), 71–81, doi:10.1007/BF02296254, 1994.

Lauter, E. A. and Schaening, B.: On the low-latitude boundary of the winter anomaly of ionospheric absorption, J. Atmos. Terr. Phys., 32, 1619–1624, 1970.

Lauter, E. A., Taubenheim, J., and Von Cossart, G.: Monitoring middle atmosphere processes by means of ground-based low-frequency radio wave sounding of the D-region, J. Atmos. Terr. Phys., 46, 775–780, 1984.

Madden, R. A.: Further evidence of traveling planetary waves, J. Atmos. Sci., 35, 1605–1618, 1978.

Mertens, C. J., Schmidlin, F. J., Goldberg, R. A., Remsberg, E. E., Pesnell, W. D., Russell, J. M., Mlynczak, M. G., Lopez-Puertas, M., Wintersteiner, P. P., Richard, H., Picard, R. H., Winick, J. R., and Gordley, L. L.: SABER observations of mesospheric temperatures and comparisons with falling sphere measurements taken during the 2002 summer MaCWAVE campaign, Geophys. Res. Lett., 31, L03105, doi:10.1029/2003GL018605, 2004.

Mitchell, N. J., Middleton, H. R., Beard, A. G., Williams, P. J. S., and Muller, H. G.: The 16-day planetary wave in the mesosphere and lower thermosphere, Ann. Geophys., 17, 1447–1456, doi:10.1007/s00585-999-1447-9, 1999.

Pogoreltsev, A. I., Kanukhinaa, A. Yu., Suvorovaa, E. V., and Savenkovaa, E. N.: Variability of planetary waves as a signature of possible climatic changes, J. Atmos. Solar-Terr. Phys., 71(14–15), 1529–1539, Long-Term Changes and Trends in the Atmosphere-Ionosphere System, 5th IAGA/ICMA/CAWSES workshop "Long Term Changes and Trends in the Atmosphere", 2009.

Schmitter, E. D.: Remote auroral activity detection and modeling using low frequency transmitter signal reception at a midlatitude site, Ann. Geophys., 28, 1807–1811, doi:10.5194/angeo-28-1807-2010, 2010.

Taubenheim, J.: Some new aspects of the winter anomaly of ionospheric absorption, J. Atmos. Terr. Phys., 33(9), 1481–1485, 1971.

Wait, J. R. and Spies, K. P.: Characteristics of the Earth-ionosphere waveguide for VLF radio waves, NBS Tech. Note, 300, 1964.